Available online at www.sciencedirect.com
SCIENCE DIRECT
International Journal of Heat and Mass Transfer 49 (2006) 3547–3554
International Journal of HEAT and MASS TRANSFER
www.elsevier.com/locate/ijhmt

Thermodynamic modelling of a solid state thermoelectric cooling device: Temperature–entropy analysis

A. Chakraborty [a], B.B. Saha [a], S. Koyama [a], K.C. Ng [b,*]

[a] Interdisciplinary Graduate School of Engineering Sciences, Kyushu University, Kasuga-koen 6-1, Kasuga-shi, Fukuoka 816-8580, Japan
[b] Department of Mechanical Engineering, National University of Singapore, 10 Kent Ridge Crescent, Singapore 119260, Singapore

Received 13 May 2005; received in revised form 15 February 2006
Available online 5 May 2006

Abstract

This article presents the temperature–entropy analysis, where the Thomson effect bridges the Joule heat and the Fourier heat across the thermoelectric elements of a thermoelectric cooling cycle to describe the principal energy flows and performance bottlenecks or dissipations. Starting from the principles of thermodynamics of thermoelectricity, differential governing equations describing the energy and entropy flows of the thermoelectric element are discussed. The temperature–entropy (T–S) profile in a single Peltier element is pictured for temperature dependent Seebeck coefficient and illustrated with data from commercial available thermoelectric cooler.

1. Introduction

The basic thermoelectric effects such as Peltier, Joule and Thomson were discovered and their macroscopic thermodynamic understanding was achieved between the 1820s and the 1850s. The interest in thermoelectric cooler was renewed in the middle of the 20th century when it was discovered that doped semiconductors were made for better thermoelectric materials than metals [1,2]. The use of semiconductors in thermoelectric refrigeration was proposed [3] using materials of high mean atomic weights and high thermoelectric powers. The relationship between cooling capacity and the coefficient of performance (COP) was examined for a single stage thermoelectric cooling unit with respect to a given temperature difference between the hot and cold junctions, and the design equations and performance graphs were presented [4]. In 1948, using the Onsager reciprocal relationship [5] the thermoelectric effects for the thermoelectric device are clearly presented [6] and the Thomson effect along the thermoelectric arm is demonstrated [6]. An earlier but important development is the theoretical formulation of irreversible thermodynamics [7], which assisted the progress of understanding thermoelectric coolers. Tolman and Fine [8] introduced the mathematical framework of entropy production or generation by irreversible processes that take place inside the system. They computed the rate of irreversible entropy production within two thermoelectric wires by considering the degradation of energy accompanying the joule heating effect and the irreversible flow of heat along the thermoelectric arms. These pioneer works have led to a plethora of recent publications in the area of thermoelectrics [9–15].

In 1990, a new interest in the study of irreversible processes in thermoelectric for refrigeration was reported by Hasse [9], and Yamanashi [10] elaborated a new optimization for designing the thermoelectric coolers using a dimensionless entropy flow approach. The study involving the interface effects of thermoelectric micro-refrigerators was proposed by Sungtaek and Ghosal [11], where they employed a phenomenological model to examine the behavior of thermoelectric refrigerator and modified the conventional definition of the figure-of-merit to capture the interface effects. The performances of the thermoelectric device have been discussed using the classical temperature–entropy approach [12–15] that provided a clear

* Corresponding author. Tel.: +65 772 2212; fax: +65 779 1459.
E-mail address: mpengkc@nus.edu.sg (K.C. Ng).

0017-9310/$ - see front matter © 2006 Elsevier Ltd. All rights reserved.
doi:10.1016/j.ijheatmasstransfer.2006.02.047

Nomenclature

A	cross-sectional area of thermoelectric element (m^2)	λ	thermal conductivity ($W\,m^{-1}\,K^{-1}$)
c_p	specific heat capacity ($J\,kg^{-1}\,K^{-1}$)	σ	electrical conductivity ($\Omega^{-1}\,m^{-1}$)
DT	temperature different between hot and cold junctions (K)	τ	Thomson coefficient ($V\,K^{-1}$)
I	current (amp)	π	Peltier coefficient (V)
J	current density ($amp\,m^{-2}$)	α	Seebeck coefficient ($V\,K^{-1}$)
$\mathbf{J}_S$	entropy flux ($W\,m^{-2}\,K^{-1}$)	*Subscripts*	
L	thermoelectric length (m)	dissip	dissipation
Q	heat or energy (W)	max	maximum value
S_{gen}	entropy generation ($W\,m^{-3}\,K^{-1}$)	H	hot junction
T	temperature (K)	L	cold junction
t	time (s)	F	Fourier heat
x	co-ordinate along X-axis (–)	J	Joule heat
ρ	density ($kg\,m^{-3}$)	T	Thomson heat

understanding as to how the electrical energy input has been utilized to produce the useful cooling, as well as how they have been consumed by the dissipative effects.

In this paper, the authors review the irreversible thermodynamic formulations for the temperature–entropy analysis of thermoelectric coolers with a special emphasis on the temperature dependency of Seebeck coefficient and hence, leading to the inclusion of the Thomson heat which has not been considered previously [12–14]. This new approach completes the physics of thermoelectric cooling where all thermoelectric effects are added to form the temperature–entropy relationship such that energy dissipation due to Joule, Fourier and Thomson heats are captured.

2. Theory

The thermoelectric effects such as Seebeck, Peltier and Thomson effects are related to the transformation of thermal into electrical energy, and vice versa. The absorption of Thomson heat in the interior of a thermally non-uniform hot conductor has been reported to be the additive superposition of two effects: firstly, a part of Thomson effect is the internal Peltier effect which is caused by the non-equilibrium electron distribution functions in a thermally non-uniform conductor, and secondly, the other part of heat is absorbed due to current flow against the drift potential difference [16]. When an electric field is applied to a thermoelectric device, the irreversible processes which are occurred in a thermoelectric elemental are: (i) electric conduction (electric current due to an electric potential gradient), (ii) heat conduction (heat flow due to a temperature gradient), (iii) a cross effect (electric current due to a temperature gradient) [5], and (iv) the appropriate reciprocal effect (heat flow due to an electric potential gradient) [5].

The refrigeration capability of a semiconductor material depends on parameters such as the Peltier effect, Joule heat, Thomson heat and material's physical properties over the operational temperatures between the hot and cold ends. A thermoelectric device as shown in Fig. 1(a) is composed of p-type and n-type thermoelectric elements such as Bi_2Te_3 and these are connected electrically in series and thermally in parallel. The thermoelectric cooling is generated by passing a direct current through one or more pairs of n- and p-type thermoelements, the temperature of cold reservoir decreases because the electrons and holes pass from the

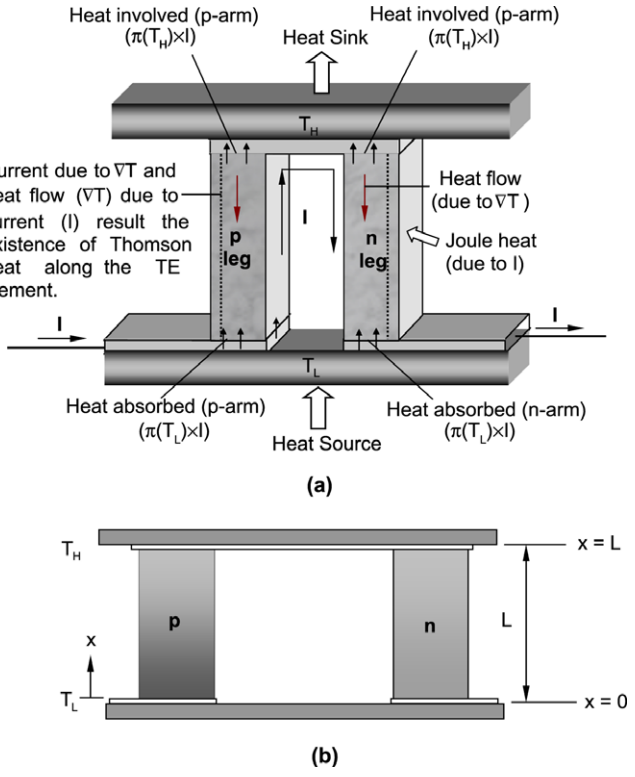

Fig. 1. The schematic view of a thermoelectric cooler.

low energy level in p-type material through the interconnecting conductor to the higher energy level in the n-type material. Similarly, the arrival of electrons and holes in the opposite ends result in an increase of energy level and hence, an increase in the local temperature forming the hot junction. When a temperature differential is established between the hot and cold junctions, a Seebeck voltage is generated and the voltage is directly proportional to the temperature differential. When current is applied to a thermoelectric element, thermal energy is generated or absorbed at the junction due to Peltier effect. The Peltier heat exchange between the metal and semiconductor (both the n- and p-type) is illustrated in Fig. 1(a). The Seebeck coefficient depends on temperature and this is different at different places along the TE material [17]. The thermoelectric element is a combination of as a series of many small Peltier junctions [dotted line as shown in Fig. 1(a)] and each of which individually generates or absorbs heat. This is called Thomson power evolved per unit volume. In Thomson effect, the heat is absorbed or evolved when current flows in a thermoelectric element with a temperature gradient and this effect is proportional to both the electric current and the temperature gradient. The Thomson effect occurs along the thermoelectric element, arising from the gradients of Seebeck coefficient and the local temperature. As all thermoelectric effects are caused by coupling between charge transport and heat transport, the quantification of these transports can be evaluated using the mass, energy and entropy equations, forming rigorous thermodynamic frameworks, which are described in the following section.

3. Energy and entropy balance

The energy balance of a bulk thermoelectric device where an electric current and a heat current flow parallel from the p-leg to the n-leg (or from the n-leg to the p-leg) depending on the direction of current in presence of an applied electric field, is given by [1,2]

$$\rho c_p \frac{\partial T}{\partial t} = \nabla \cdot (\lambda \nabla T) + \frac{J^2}{\sigma} - J\tau \nabla T. \tag{1}$$

Lord Kelvin first proposed the quasi-thermodynamic method [6] of the thermoelectric effects to prove the validity of the relationships $-\tau = \frac{\pi}{T} - \frac{\mathrm{d}\pi}{\mathrm{d}T}$ and $\pi = \alpha T$ where τ is the Thomson coefficient, π is the Peltier heat and α is the Seebeck coefficient. Hence the gradient of Peltier heat $\nabla\pi$ $\left(= \nabla\pi|_{\mathrm{T}} + \frac{\partial \pi}{\partial T} \cdot \nabla T\right)$ splits up into two parts [7]: The first presents the heat effect even in the absence of temperature gradient and the second part indicates the heat effect due to a temperature gradient. Using Eq. (1), the energy balance of a thermoelectric element is written as

$$\rho c_p \frac{\partial T}{\partial t} = \nabla \cdot (\lambda \nabla T) + \frac{J^2}{\sigma} - JT\frac{\partial \alpha}{\partial T} \cdot \nabla T + JT\nabla\alpha|_{\mathrm{T}}. \tag{2}$$

Following the Gibbs law and energy conservation within a control volume [7], the basic entropy balance equation can be expressed as [15]

$$\frac{\partial(\rho s)}{\partial t} = \nabla \cdot \left(-\frac{\lambda \nabla T}{T} + \alpha J\right) + \left[\frac{J^2}{T\sigma} - \lambda \nabla T \cdot \nabla\left(\frac{1}{T}\right) + J \cdot \nabla\alpha|_{\mathrm{T}}\right], \tag{3}$$

where the first terms indicate the entropy flux $\mathbf{J}_{\mathrm{S}}$ ($\mathrm{W\,m^{-2}\,K^{-1}}$) and the second terms are entropy generation S_{gen} ($\mathrm{W\,m^{-3}\,K^{-1}}$) and these are expressed as

$$\mathbf{J}_{\mathrm{S}} = \frac{-\lambda \nabla T}{T} + \alpha J \tag{4}$$

and

$$S_{\mathrm{gen}} = \frac{J^2}{T\sigma} - \lambda \nabla T \cdot \nabla\left(\frac{1}{T}\right) + J \cdot \nabla\alpha|_{\mathrm{T}}. \tag{5}$$

With the boundary conditions indicated in Fig. 1(b), for thermoelectric legs of length L ($0 \leqslant x \leqslant L$), the one-dimensional energy balance equation for p- and n-legs becomes

$$(\rho c_p)\frac{\partial T(x,t)}{\partial t} = \lambda \frac{\partial^2 T(x,t)}{\partial x^2} + \frac{J^2}{\sigma} - \tau J \cdot \frac{\partial T(x,t)}{\partial x}. \tag{6}$$

Putting boundary conditions (at $x = 0$, $T = T_{\mathrm{L}}$ and $x = L$, $T = T_{\mathrm{H}}$), the steady state analytical solution of Eq. (6) is written as $T = T_{\mathrm{L}} + \frac{\rho J}{\tau}x + \frac{\left(\mathrm{DT} - \frac{\rho J L}{\tau}\right)}{\left(\mathrm{e}^{\left(\frac{\tau J}{\lambda} L\right)} - 1\right)}\left(\mathrm{e}^{\left(\frac{\tau J}{\lambda} x\right)} - 1\right)$, where DT indicates the temperature difference between the hot and cold junctions, i.e., $\mathrm{DT} = T_{\mathrm{H}} - T_{\mathrm{L}}$. Hence the temperature gradient along x direction is given by

$$\frac{\mathrm{d}T}{\mathrm{d}x} = \frac{\rho J}{\tau} + \exp\left(\frac{\tau J}{\lambda}x\right)\left[\frac{\left(\mathrm{DT} - \frac{\rho J L}{\tau}\right)\frac{\tau J}{\lambda}}{\left(\exp\left(\frac{\tau J}{\lambda}L\right) - 1\right)}\right] \quad \text{or}$$

$$-\lambda A \frac{\mathrm{d}T}{\mathrm{d}x} = -\frac{\lambda \rho I}{\tau} + \frac{\left(-\frac{\lambda A \mathrm{DT}}{L} + \frac{\lambda \rho I}{\tau}\right)\frac{\tau I L}{\lambda A}}{\left(\exp\left(\frac{\tau I L}{\lambda A}\left(1 - \frac{x}{L}\right)\right) - \exp\left(-\frac{\tau I L}{\lambda A}\frac{x}{L}\right)\right)}, \tag{7}$$

where $I = JA$. Defining Fourier heat $Q_{\mathrm{F}} = \frac{\lambda A \mathrm{DT}}{L}$, Joule heat $Q_{\mathrm{J}} = \frac{\rho I^2 L}{A}$, Thomson heat $Q_{\mathrm{T}} = I\tau\mathrm{DT}$ and $\frac{Q_{\mathrm{T}}}{Q_{\mathrm{F}}} = \frac{I\tau \mathrm{DT}}{\frac{\lambda A \mathrm{DT}}{L}} = \frac{I\tau L}{\lambda A}$. Eq. (7) is written as

$$-\lambda A \frac{\mathrm{d}T}{\mathrm{d}x} = -\frac{\lambda \rho I}{\tau} + \frac{\left(-Q_{\mathrm{F}} + \frac{\lambda \rho I}{\tau}\right)\frac{Q_{\mathrm{T}}}{Q_{\mathrm{F}}}}{\left(\exp\left(\frac{Q_{\mathrm{T}}}{Q_{\mathrm{F}}}\left(1 - \frac{x}{L}\right)\right) - \exp\left(-\frac{Q_{\mathrm{T}}}{Q_{\mathrm{F}}}\frac{x}{L}\right)\right)}. \tag{8}$$

At cold junction ($x = 0$)

$$-\lambda A \left.\frac{\mathrm{d}T}{\mathrm{d}x}\right|_{x=0} = -\frac{\lambda \rho I}{\tau} + \frac{\left(-Q_{\mathrm{F}} + \frac{\lambda \rho I}{\tau}\right)\frac{Q_{\mathrm{T}}}{Q_{\mathrm{F}}}}{\left(\exp\left(\frac{Q_{\mathrm{T}}}{Q_{\mathrm{F}}}\right) - 1\right)} = \frac{\frac{Q_{\mathrm{T}}}{Q_{\mathrm{F}}}}{\left(\exp\left(\frac{Q_{\mathrm{T}}}{Q_{\mathrm{F}}}\right) - 1\right)}\left(-Q_{\mathrm{F}} + \frac{\lambda \rho I}{\tau}\right) - \frac{\lambda \rho I}{\tau}.$$

Using the expansion of $\frac{\frac{Q_T}{Q_F}}{\left(\exp\left(\frac{Q_T}{Q_F}\right)-1\right)}$

$$\frac{\frac{Q_T}{Q_F}}{\left(\exp\left(\frac{Q_T}{Q_F}\right)-1\right)} = 1-\frac{1}{2}\frac{Q_T}{Q_F}+\frac{1}{6}\frac{1}{2}\left(\frac{Q_T}{Q_F}\right)^2-\frac{1}{360}\frac{1}{2}\left(\frac{Q_T}{Q_F}\right)^4+\cdots,$$

$$\left(-Q_F+\frac{\lambda\rho I}{\tau}\right)\frac{\frac{Q_T}{Q_F}}{\left(\exp\left(\frac{Q_T}{Q_F}\right)-1\right)} = \left(-Q_F+\frac{\lambda\rho I}{\tau}\right)\times 1-\frac{1}{2}\frac{Q_T}{Q_F}+\frac{1}{6}\frac{1}{2}\left(\frac{Q_T}{Q_F}\right)^2-\frac{1}{360}\frac{1}{2}\left(\frac{Q_T}{Q_F}\right)^4+\cdots$$

After rearranging,

$$-\lambda A\left.\frac{dT}{dx}\right|_{x=0} = \left[-Q_F-\frac{1}{2}Q_T-\frac{1}{2}Q_J\right]+\frac{1}{6}\left[\frac{1}{2}\frac{Q_T^2}{Q_F}+\frac{1}{2}\frac{Q_JQ_T}{Q_F}\right]-\frac{1}{360}\left[\frac{1}{2}\frac{Q_T^4}{Q_F^3}+\frac{1}{2}\frac{Q_JQ_T^3}{Q_F^3}\right]+\cdots,$$

$$-\lambda A\left.\frac{dT}{dx}\right|_{x=0} = \left[-Q_F-\frac{1}{2}Q_T-\frac{1}{2}Q_J\right]+\frac{1}{6}\left[\frac{1}{2}\frac{Q_T^2}{Q_F}+\frac{1}{2}\frac{Q_JQ_T}{Q_F}\right]. \quad (9)$$

Similarly at hot junction (removing all higher order terms)

$$-\lambda A\left.\frac{dT}{dx}\right|_{x=L} = \left[-Q_F+\frac{1}{2}Q_T+\frac{1}{2}Q_J\right]+\frac{1}{6}\left[\frac{1}{2}\frac{Q_T^2}{Q_F}+\frac{1}{2}\frac{Q_JQ_T}{Q_F}\right]. \quad (10)$$

The higher order terms of Eqs. (9) and (10) indicate the interactions of Joule, Thomson and Fourier effects.

The transport of energy along the thermoelectric arm is

$$\begin{aligned} Q(x) &= \alpha IT(x)-\lambda A\frac{dT}{dx},\\ Q(x) &= \alpha IT(x)-\frac{\lambda\rho I}{\tau}+\frac{\left(-Q_F+\frac{\lambda\rho I}{\tau}\right)\frac{Q_T}{Q_F}}{\left(\exp\left(\frac{Q_T}{Q_F}\left(1-\frac{x}{L}\right)\right)-\exp\left(-\frac{Q_T}{Q_F}\frac{x}{L}\right)\right)}. \end{aligned} \quad (11)$$

The entropy flux along the thermoelectric arm is simply obtained by the ratio of $Q(x)$ to $T(x)$, i.e.,

$$\mathbf{J}_S(x) = \alpha I-\frac{\lambda\rho I}{\tau T(x)}+\frac{\left(-Q_F+\frac{\lambda\rho I}{\tau}\right)\frac{Q_T}{Q_F}}{\left(\exp\left(\frac{Q_T}{Q_F}\left(1-\frac{x}{L}\right)\right)-\exp\left(-\frac{Q_T}{Q_F}\frac{x}{L}\right)\right)}\frac{1}{T(x)}. \quad (12)$$

Eq. (12) represents the entropy flow along the thermoelectric arm and captures the contributions of Peltier, Joule, Fourier and Thomson heats. Joule contribution extracts the entropy produced by the flow of current. Fourier heat also removes the flow of energy due to the transportation of heat from hot to cold junctions. The Thomson heat supplies the flow of entropy in the particles of the thermoelectric element, so the Thomson heat may be referred to as 'the specific heat of electricity' [6].

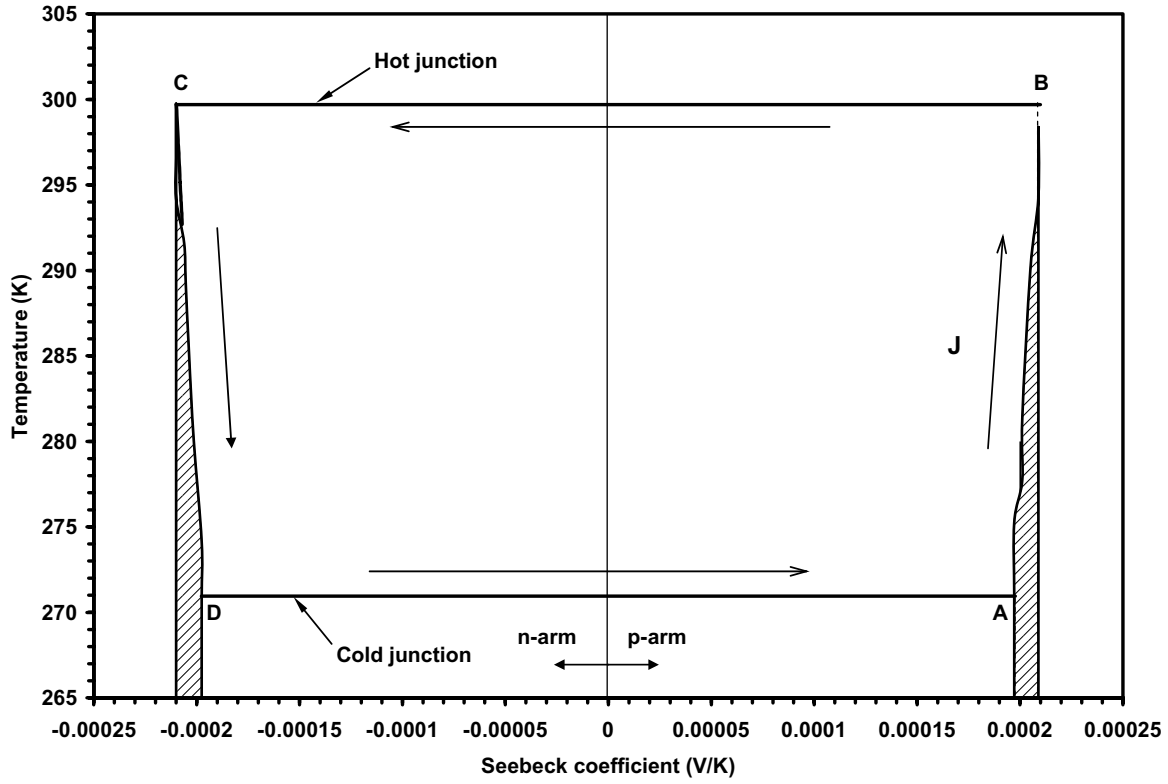

Fig. 2. T–α diagram of a thermoelectric pair.

4. Temperature–entropy (*T*–*S*) diagram and analysis

From the work of Carnot and Clasius, Kelvin deduced that the reversible heat flow discovered by Peltier must have entropy associated with it. It has been shown that the coefficient discovered by Seebeck was a measure of entropy associated with electric current [2]. With the general formulation of Eqs. (6) and (12), a temperature–entropy flux diagram can now be drawn as a function of the spatial length of the p- and n-elements of thermoelectric. Prior to the temperature–entropy diagram, the authors plot the temperature–Seebeck coefficient or T–α for the operation of a thermoelectric cooler, which is shown in Fig. 2. For an ideal thermoelectric device, the Seebeck (α) coefficient is constant and the heat flux at the hot and cold junctions are given by αJT_i where the subscript i refers either to the hot or cold junction. Thus, the temperature Seebeck coefficient (T-α) plot is simply a simple rectangle. However, the effect of temperature on the Seebeck coefficient (α) induces the dissipative losses along the p- and n-legs of thermoelectric couples and an indication of these losses are shown by the shaded area on the T–α plot, as shown in Fig. 2, in which the physical properties of the bismuth telluride thermoelectric pairs are used. The two isotherms are the hot and cold junctions whilst the inclined lines indicate the effect of temperature on the α values when the current (I) travels along the p- and n-legs. The physical properties of the bismuth telluride thermoelectric pairs used in the computation are as listed in Table 1.

Table 1
Physical parameters of a single thermoelectric couple

Property	Value
Hot junction temperature, T_H	300 K
Cold junction temperature, T_L	270 K
Thermoelectric element length, L	1.15×10^{-3} m[a]
Cross-sectional area, A	1.96×10^{-6} m^2 [a]
Electrical conductivity, σ	97087.38 Ω^{-1} m^{-1} [a]
Seebeck coefficient, α, $\alpha(T)=\alpha_0+\alpha_1\ln(T/T_0)$	$\alpha_0=210\times10^{-6}$ V/K, $\alpha_1=120\times10^{-6}$ V/K, $T_0=300$ K [17]
Thermal conductivity, λ	1.70 W m^{-1} K^{-1} [a]
Thomson coefficient, τ	6.7×10^{-5} V/K [18]

[a] Melcor thermoelectric catalogue, MELCOR CORPORATION, 1040 Spruce Street, Trenton, NJ 08648, USA. Web site: www.melcor.com.

For thermodynamic consistency, the temperature–entropy (or temperature–entropy flux) plot is highlighted to demonstrate how the electric energy input is distributed in the thermoelectric p- and n-elements, i.e., identifying the useful effects and the dissipative losses of a thermodynamic cycle. For an optimum current operation of the thermoelectric cooler, for example, the entropy generations or energy dissipations due to the conduction heat transfer and the Joule heating effect along are manifested by enclosed polygonal areas "k–l–u–r–d–c–k" and "j–i–n–q–a–b–j" of Fig. 3. The shaded areas under trapezoidal corresponds to the dissipation from the temperature effects on the Seebeck coefficient. It is noted that all entropy generation (internal and external) have the consequence

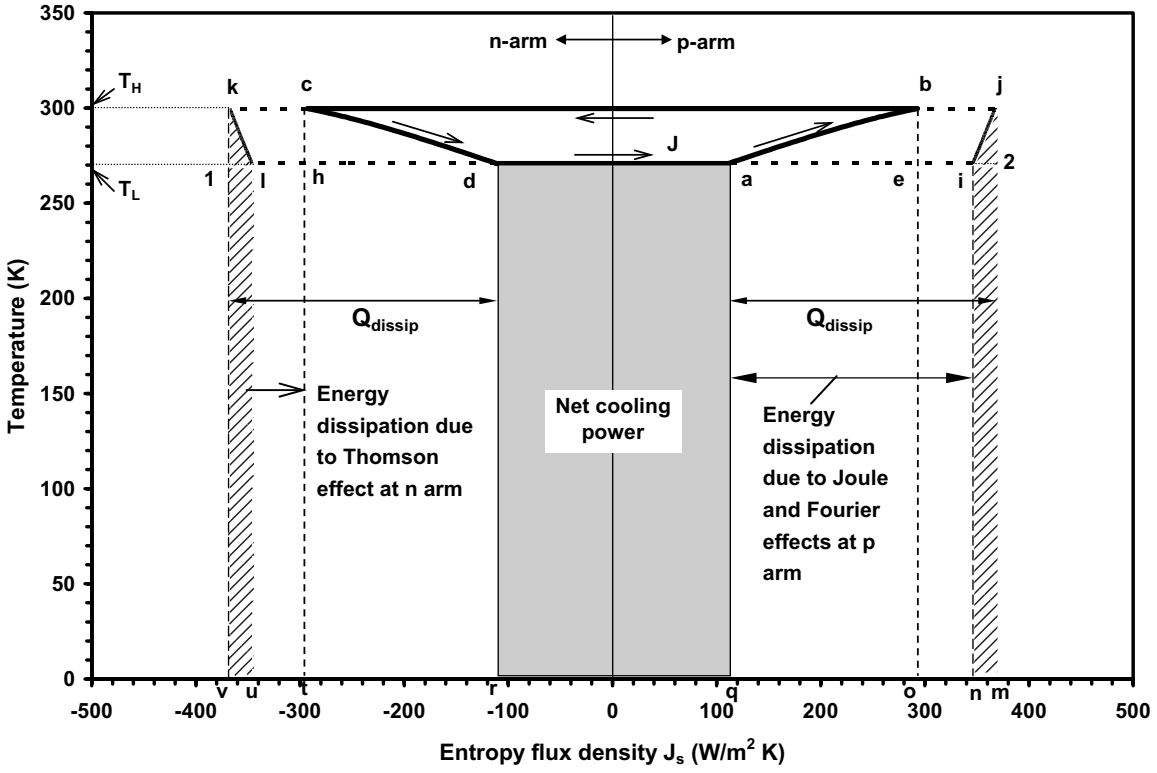

Fig. 3. Temperature–entropy flux diagram for the thermoelectric cooler at the maximum coefficient of performance identifies the principal energy flows.

Table 2
Description of close loop a–b–c–d–a (Fig. 3)

Thermodynamic process	Description
a–b	This process is developed along p-arm of the thermoelectric pair. Points a and b are the states at the ends of the thermoelement of which the temperatures are T_L and T_H, respectively (as current density J flows from p-arm to n-arm). The process a–b can not be adiabatic because it absorbs heat due to the Thomson effect which depends on the Seebeck coefficient of the thermoelectric element. The areas beneath the a–b process represent dissipation due to heat conduction, and heat absorbed by the Thomson effect. Area 2–i–j represents the energy dissipation due to Seebeck coefficient, which varies along the thermoelectric p-arm
b–c	This process represents the heat exchange between system and medium (environment) which occurs at the union between p-arm and n-arm at temperature T_H
c–d	The process c-d is developed along n-arm, where points c and d are at the ends of the thermoelement whose temperature are T_H and T_L. The areas beneath c–d process indicate heat losses due to dissipation. If this process is adiabatic, the Thomson effect would be null. Area 1–l–k indicates the energy losses due to the Thomson heat along the n-arm
d–a	This process represents the heat exchange between the system and the heat load at isothermal condition; however, it occurs in the physic union between thermoelectric elements at temperature T_L

of reducing the cooling effect, where the cooling capacity is represented by the shaded rectangle area "a–d–r–q". Within the internal framework of an adiabatic chiller, the cycle "a–b–c–d" operates in an anti-clockwise manner, comprising two isotherms b–c and d–a, as well as two adiabats a–b and c–d. Table 2 elaborates in details the processes of the thermoelectric cooler. Thus, the temperature–entropy flux diagram provides at a glance, how the real chiller cycle of thermoelectric is inferior to the ideal Carnot cycle by capturing the key losses and useful effects in the cycle. From the perspective of the same energy input to the thermoelectric, the Carnot efficiency is simply given by

$$\mathrm{COP}_{\mathrm{Carnot}} = \mathrm{Area}(1\mathrm{vm}2)/\mathrm{Area}(12\mathrm{jk}) = T_L/\Delta T.$$

Based on the process paths of the temperature–entropy flux diagram, the heat transfers at the cold (process d–a) and hot (process b–c) reservoirs can be easily tallied with respect to the enclosed rectangular areas and these areas correspond to the parameters such as the Peltier cooling or heating, the Joule, Fourier and the Thomson heat. At $x = 0$ and ignoring the contributions from the higher order terms emanating from the expansion of the exponentials, the cooling capacity at the cold junction can be shown to be $Q_L = |\mathrm{Area}(\mathrm{adrq})| = \alpha I T_L - \lambda A \frac{dT}{dx}\big|_{x=0} = \alpha I T_L + [-Q_F - \frac{1}{2}Q_T - \frac{1}{2}Q_J]$ (neglecting higher order terms in Eq. (9)) and similarly, at $x = L$, the heating capacity at the hot junction is $Q_H = |\mathrm{Area}(\mathrm{bcto})| = \alpha I T_H - \lambda A \frac{dT}{dx}\big|_{x=L} = \alpha I T_H + [-Q_F + \frac{1}{2}Q_T + \frac{1}{2}Q_J]$ (neglecting higher order terms in Eq. (10)). Thus, the power input (P) to the thermoelectric becomes $Q_H - Q_L$, i.e., $P = \alpha I(T_H - T_L) + Q_J + Q_T$.

For the purpose of concise presentation of the COP-entropy map at the cold junction, the COP and the non-dimensional entropy fluxes of $\mathbf{J}_S\ (x = 0)/\mathbf{J}_{S,\max}\ (x = 0)$ are employed and these are shown in Fig. 4. These two "kidney-shape" curves, where one (solid lines) indicates the effect of Thomson heat at different current fields and the other (dotted lines) does not possess the Thomson heat effect, are traced in the clockwise directions along with four salient operational points of a thermoelectric cooler. For

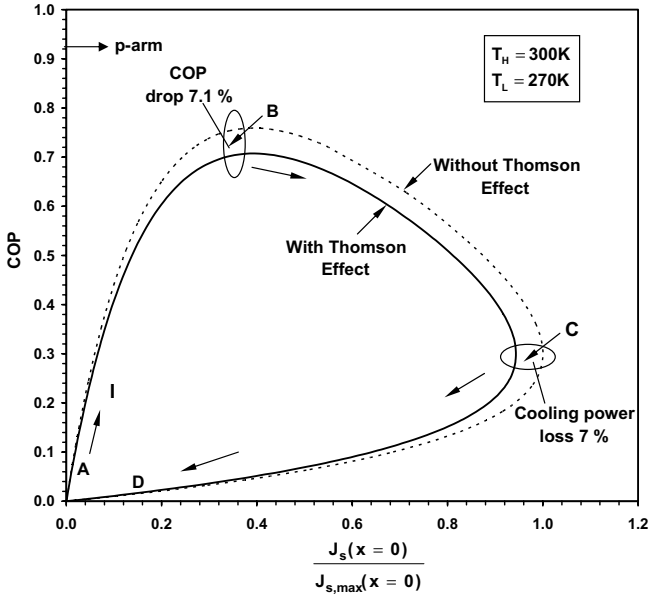

Fig. 4. Characteristics performance curve of the thermoelectric cooler. COP is plotted against entropy flux for the both n- and p-legs.

example, as indicated on each operational loop, (i) Point "A" indicates the COP at its low current limit in which the Thomson effect is negligible, (ii) Point "B" is the maximum COP at the optimum current flow, where the performance drops 7.1% as a result of Thomson heat effect at the same cooling power, (iii) Point "C" denotes the maximum entropy flux or output power, where the cooling capacity is decreased about 7% due to Thomson heat and (iv) Point "D" represents the vanishing COP at the higher current limit in which there is no Thomson effect. When the Thomson coefficient $\tau = 0$, there is no loss but if $\tau < 0$, the cooling capacity as well as the performance of the thermoelectric cooler is improved. So the cooling efficiency of a thermoelectric cooler can be improved not only by increasing the figure-of-merit of the thermoelectric materials but also by taking advantage of the Thomson effect [18].

Fig. 5 shows an enlarged temperature–entropy flux diagram where the adiabats linking the two isotherms are

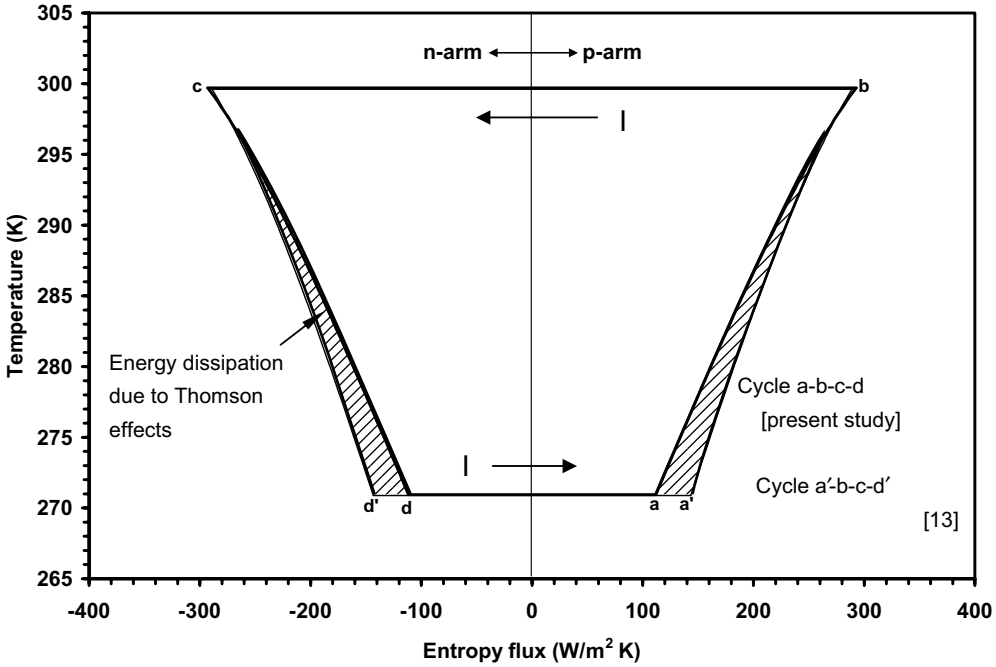

Fig. 5. Temperature–entropy flux diagram for the thermoelectric pair at the optimum current flow by the present study (Area abcd) and the other researcher (Area a′bcd′ [13]).

represented by paths "a–b" and "c–d". The shaded area along the adiabats represents the entropy generation arising from the Thomson effect, an effect that has been ignored by previous work [13,14] and consequently, the cooling capacity of thermoelectric would be reduced. For a better appreciation of the dissipative effects in the thermoelectric element, the temperature–entropy generation (T–S_{gen}) plot is adopted. As shown in Fig. 6, two major dissipative mechanisms in the thermoelectric are clearly identified, namely, (i) the Joule heat dissipation occurs along the two sides of thermoelectric arms, depicted by the enclosed area a–g–h–d, and (ii) a smaller loss arising from the heat conduction

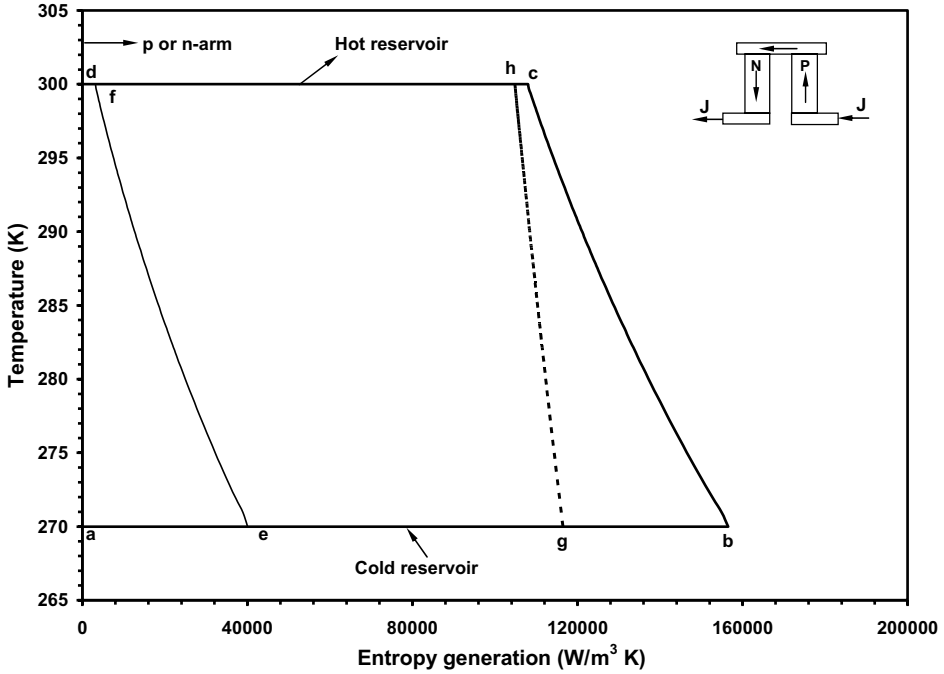

Fig. 6. Temperature–entropy generation diagram of a thermoelectric cooler at optimum cooling power. Area (abcd) is the total heat dissipation along the thermoelectric element, where area (aefd) is the irreversibility due to heat conduction and area (aghd) indicates the entropy generation due to joule effect.

effect along the thermoelectric element, denoted by area a–e–f–d, and the combined entropy generation or losses are given by the area a–b–c–d.

5. Conclusions

The temperature–entropy flux diagram has been successfully demonstrated in the analysis of the cooling cycle of a thermoelectric element. The area under the process paths indicates how the energy input has been consumed by the presence of both the reversible (Peltier, Seebeck and Thomson) and the irreversible (Joule and Fourier) effects. The similarity between the Seebeck coefficient and entropy flux of the thermoelectric element has also been depicted where the T–α diagram would be equivalent to the Carnot cycle if the thermoelectric arms are assumed adiabatic. However, the temperature dependency of Seebeck coefficient is revealed in a real T–α cycle. Lastly, the presence of Thomson heat has been incorporated in the performance estimation of a thermoelectric cooler and in contrary to previous studies, its contribution to the total losses at the cold junction is estimated to be about 5–7%.

References

[1] D.M. Rowe (Ed.), CRC Handbook of Thermoelectrics, CRC Press, Boca Raton, FL, 1995.
[2] G.S. Nolas, J. Sharp, H.J. Goldsmid, Thermoelectrics Basic Principles and New Materials Developments, Springer, Germany, 2001.
[3] H.J. Goldsmid, R.W. Douglas, The use of semiconductors in thermoelectric refrigeration, Br. J. Appl. Phys. (1954) 386–390.
[4] J.E. Parrot, A.W. Penn, The design theory of thermoelectric cooling elements and units, Solid State Electron. 3 (1961) 91–99.
[5] L. Onsager, Reciprocal relations in irreversible processes, Phys. Rev. 37 (1931) 405–426.
[6] H.B. Callen, The application of Onsager's reciprocal relation to thermoelectric, thermomagnetic, and galvanometric effects, Phys. Rev. 15 (11) (1948) 1349–1358.
[7] S.R. De Groot, P. Mazur, Non-equilibrium Thermodynamics, North-Holland Pub Co., Amsterdam, 1962.
[8] R.C. Tolman, P.C. Fine, On the irreversible production of entropy, Rev. Mod. Phys. 20 (1) (1948) 51–77.
[9] R. Hasse, Thermodynamics of Irreversible Processes, Dover Publications Inc., New York, 1990.
[10] M. Yamanashi, A new approach to optimum design in thermoelectric cooling systems, J. Appl. Phys. 80 (9) (1996) 5494–5502.
[11] J.U. Sungtaek, U. Ghoshal, Study of interface effects in thermoelectric micro-refrigerators, J. Appl. Phys. 88 (7) (2000) 4135–4139.
[12] A. Arenas, J. Vazquez, M.A. Sanz-Bobi, R. Palacios, Performance of a thermoelectric module using the thermodynamic relationship temperature–entropy (T–S), in: XIX Int. Conf. Thermoelectrics, Cardiff Wales, United Kingdom, August 2000.
[13] H.T. Chua, K.C. Ng, X.C. Xuan, C. Yap, Temperature entropy formulation of thermoelectric thermodynamic cycles, Phys. Rev. E 65 (2002) 1–6, 056111.
[14] X.C. Xuan, K.C. Ng, C. Yap, H.T. Chua, Temperature–entropy diagrams for multi-stage thermoelectric coolers, Semicond. Sci. Technol. 18 (2003) 273–277.
[15] A. Chakraborty, K.C. Ng, Thermodynamic formulation of temperature–entropy diagram for the transient operation of a pulsed thermoelectric cooler, Int. J. Heat Mass Transfer 49 (2006) 1845–1850.
[16] A.I. Burshteyn, Semiconductor Thermoelectric Devices, A Heywood Book Temple Press Books Ltd., London, 1964.
[17] W. Seifert, M. Ueltzen, E. Müller, One dimensional modeling of thermoelectric cooling, Phys. Status Solidi (a) 194 (1) (2002) 277–290.
[18] J. Chen, Z. Yan, The influence of Thomson effect on the maximum power output and maximum efficiency of a hermoelectric generator, J. Appl. Phys. 79 (1996) 8823–8828.